

Short Communication

Electrical Properties of a Solid Electrolyte Based on In₂O₃-doped CaZrO₃ Prepared by High-pressure Sintering

Jiazhuo Peng^{1,2}, Heping Li^{1,*}, Dongsheng Ren^{1,2}, Pan Wang¹

¹ Key Laboratory of High-temperature and High-pressure Study of the Earth's Interior, Institute of Geochemistry, Chinese Academy of Sciences, Guiyang, 550081, China

² University of Chinese Academy of Sciences, Beijing, 100049, China

Corresponding author. Institute of Geochemistry, Chinese Academy of Sciences, Guiyang, 550081, China

*E-mail: liheping@vip.gyig.ac.cn

Received: 15 January 2020/ Accepted: 10 March 2020 / Published: 10 May 2020

The present work provides a simple and effective route for the production of high quality CaZr_{0.9}In_{0.1}O_{3-δ} (CZI) at relatively low temperature by using high-pressure sintering method. A comparison of structure and conductivity between pressureless sintered CZI (PL-CZI) and high-pressure sintered CZI (HP-CZI) ceramics was carried out using X-ray diffraction as well as scanning electron microscope and AC impedance spectroscopy. In addition, the electrochemical response and sealing performance of the CZI ceramics in high-pressure hydrothermal fluids were tested in a self-designed autoclave. The introduction of pressure during sintering endowed the CZI ceramic with high conductivity, excellent mechanical performance and favorable corrosion resistance; these traits make the HP-CZI ceramic an ideal electrolyte material for hydrogen sensors in high-pressure hydrothermal systems.

Keywords: High-pressure sintering; Proton conductor; CaZrO₃; Ceramic; Electrical properties

1. INTRODUCTION

Hydrogen is typically considered a master variable of high-pressure hydrothermal systems that affects the direction and magnitude of mass transfer reactions [1-4]. However, one of the most difficult issues for in-situ monitoring of hydrogen in high-pressure hydrothermal systems is a lack of suitable electrolyte materials that withstand severe mechanical, thermal, and chemical conditions [5-7].

The In₂O₃-doped CaZrO₃ based high temperature proton conductor possesses advantages such as excellent chemical stability [8], good thermal shock resistance [9] and high proton transport number

[10] that has enabled it to become an attractive electrolyte for hydrogen sensors in molten metals industry [11, 12].

However, it should be noted that very high sintering temperatures (up to 1700 °C) are required to prepare In_2O_3 -doped CaZrO_3 ceramics using conventional methods [13]; these extreme temperatures potentially lead to barium and indium evaporation [14, 15]. Furthermore, the use of materials in high-pressure hydrothermal systems is so demanding that ceramics prepared by conventional methods cannot meet the requirements. One important strategy to solve this dilemma was the development of novel methods to produce high performance materials at lower temperatures. In the present work, a new high-pressure sintering method for production of a high performance CZI ceramic is proposed and its electrical properties were studied.

2. EXPERIMENTAL

Samples of $\text{CaZr}_{0.9}\text{In}_{0.1}\text{O}_{3-\delta}$ were synthesized using a solid state reaction method with CaCO_3 (99.9%), ZrO_2 (99.95%) and In_2O_3 (99.99%) utilized as raw materials. Stoichiometric amounts of selected materials were mixed and calcined in air at 1300 °C for 12 h. The calcined powders were pressed isostatically under 200 MPa into compact cylindrical shapes which were subsequently sintered by two methods, i.e. pressureless and high-pressure sintering. A muffle furnace was used for pressureless sintering of CZI at 1600 °C for 20 h, while high-pressure sintering of CZI was performed in a DS 6×1400t cubic press at 1000 °C and 0.4 GPa for 1 h; the sample assembly is shown in Fig. 1 [16].

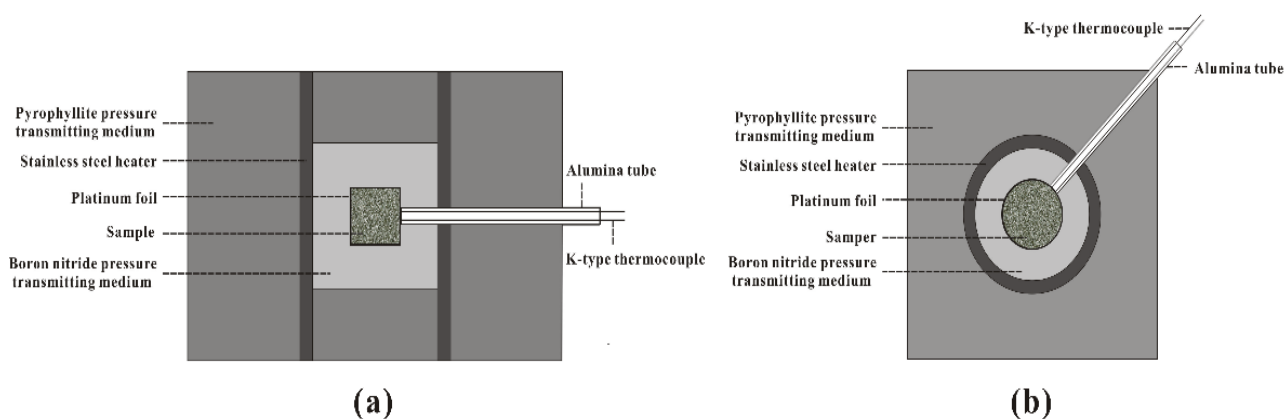


Figure 1. Section schematic diagram (a) and vertical schematic diagram (b) of the experimental assembly.

X-ray diffraction (XRD, D/Max 2200VPC, Japan) was employed to identify the crystal structures of both PL-CZI and HP-CZI ceramics before and after testing in high-pressure hydrothermal

fluids. A field-emission scanning electron microscope (FE-SEM, Sigma HD, Germany) was used to observe microstructures and element mapping of the sintered ceramics. AC impedance spectroscopy was investigated with an impedance/gain-phase analyzer (Solartron 1260, UK) in a frequency range of 1-10⁶ Hz. Finally, the high-pressure resistant together with the electrochemical response of the sintered CZI ceramics was tested in an autoclave. After grinding the sintered ceramics into a circular truncated cone, platinum electrodes were attached to both ends of the processed ceramic material and then pressed into an autoclave. Appropriate amount of deionized water was put into an autoclave; subsequent heating of the autoclave resulted in vapor pressure changes. Consequently, a gas concentration cell was formed as a result of the different hydrogen partial pressures between the outside and inside of the autoclave.

3. RESULTS AND DISCUSSION

The XRD patterns of PL-CZI and HP-CZI ceramics are shown in Fig. 2(a) and (b), respectively. The patterns exhibited pure perovskite structures were formed without secondary phases after sintering under both atmospheric and high-pressure; all diffraction peaks aligned perfectly with crystalline CaZrO₃ (JCPDS No. 76-2401) and corresponded to those previously reported[17-20]. Figure 2(c) presents the XRD spectrum of HP-CZI after ten days of testing in high-pressure hydrothermal fluids. No additional phases except the pure CaZrO₃ phase with perovskite structure were observed from the spectrum, which demonstrated that exposure to high-pressure hydrothermal systems had not changed the phase composition and indicated that the HP-CZI ceramic has excellent chemical stability [21].

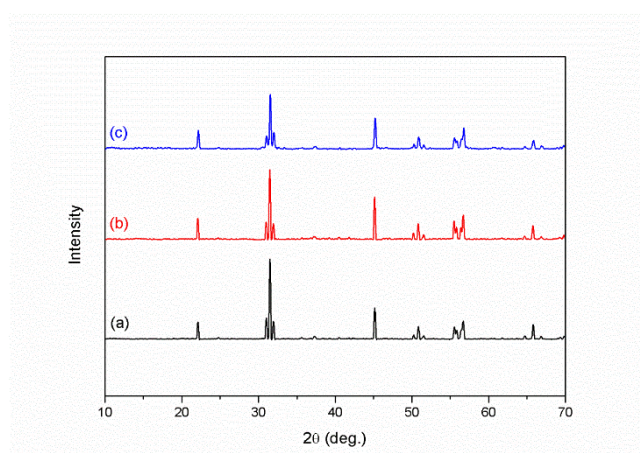


Figure 2. X-ray diffraction patterns of (a) PL-CZI ceramic as well as the HP-CZI ceramic before (b) and after (c) testing in high pressure hydrothermal fluids for ten days.

SEM micrographs and elemental mapping of the PL-CZI and HP-CZI ceramics are displayed in Fig. 3. Elements in the PL-CZI and HP-CZI samples were evenly distributed; therefore, it can be concluded that In was successfully doped into CaZrO_3 [22].

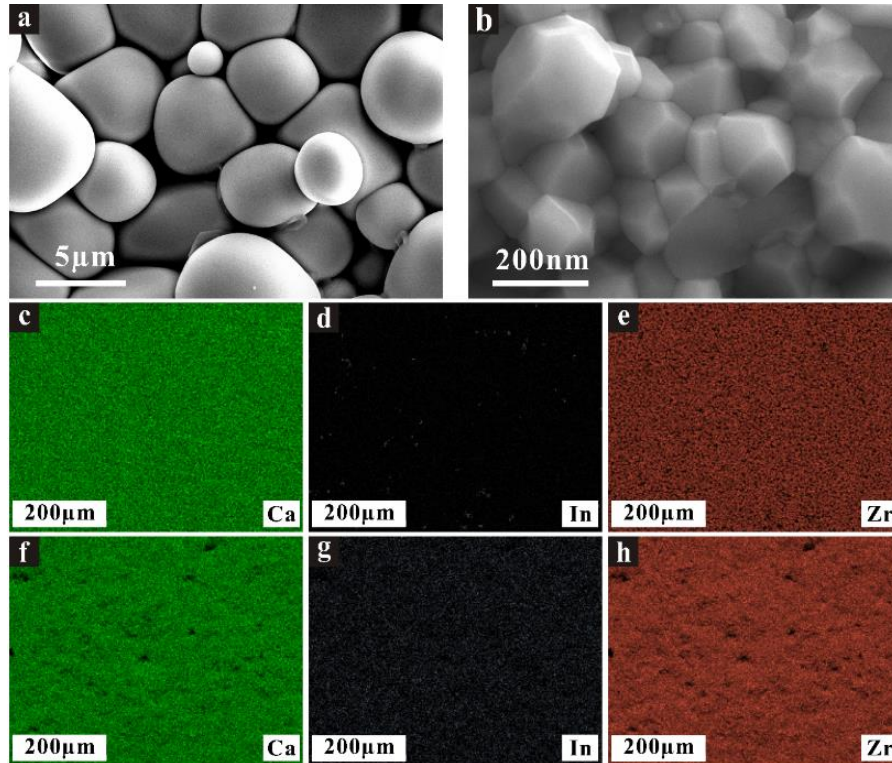


Figure 3. SEM micrographs of (a) PL-CZI ceramic and (b) HP-CZI ceramic, elemental mapping of (c)-(e) PL-CZI ceramic and (f)-(h) HP-CZI ceramic.

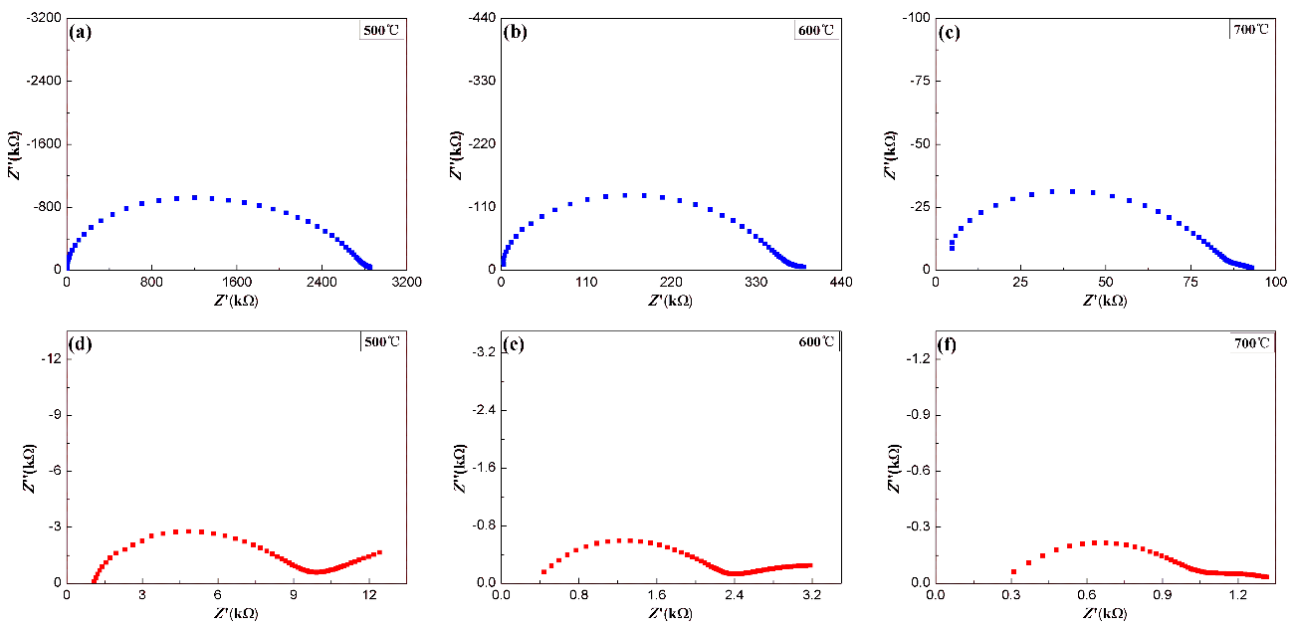


Figure 4. Selected impedance spectra of the PL-CZI ceramic (a)-(c) and HP-CZI ceramic (d)-(f) at different temperatures in ambient air.

However, some differences in their microstructures were also observed. The HP-CZI ceramic had fewer closed pores and smaller grain sizes (about 200 nm) compared to the PL-CZI ceramic (about 5 μm), showing that pressurization during sintering contributed to restraining grain growth which made the CZI ceramic more compact [23].

Figure 4 shows the selected impedance spectra of the PL-CZI and HP-CZI ceramics from 500 $^{\circ}\text{C}$ to 700 $^{\circ}\text{C}$ in ambient air; Arrhenius plots of conductivity based on the fitted data are shown in Fig. 5. At those temperatures, HP-CZI exhibited higher conductivity as compared to PL-CZI. Conventional wisdom suggests that diffusion of the proton along the grain boundary is limited by the higher potential barrier [24-26], so crystalline materials with large grain sizes should have higher conductivities due to smaller grain boundary areas [27]. However, the effect of porosity should not be ignored. High porosity increases the grain boundary area and reduces the conductivity and helps explain why the conductivity of HP-CZI is higher than PL-CZI. The conductivity of HP-CZI was 2.71×10^{-4} S/cm at 700 $^{\circ}\text{C}$; higher than the conductivity of the pressureless sintered CZI ceramic as reported by Dai et al. [28] (2.23×10^{-4} S/cm). This behavior could be attributed to a more compact microstructure of HP-CZI which reduced the grain boundary area. These results demonstrated that high-pressure sintering significantly improved the conductivity of CZI.

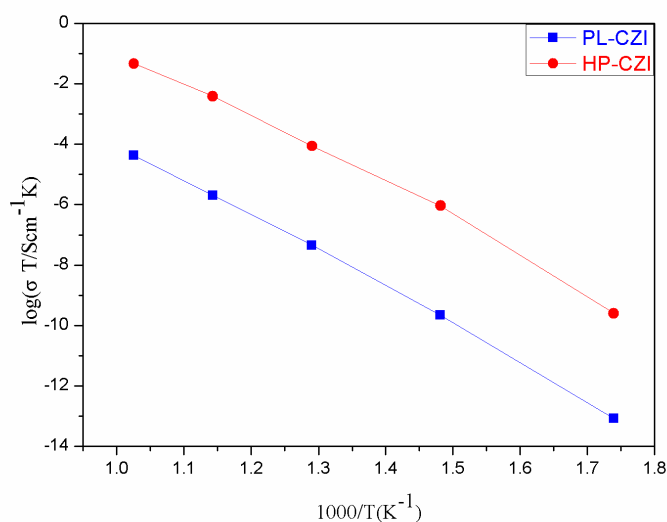


Figure 5. Arrhenius plots of conductivity of the PL-CZI and HP-CZI ceramics.

The electrochemical response together with mechanical properties of the CZI ceramics was investigated by heating a water-filled autoclave in which the CZI ceramic acted as both electrolyte and sealing material. HP-CZI could be processed into fixed shape and maintained stability even when exposed to a hydrothermal system with temperatures up to 400 $^{\circ}\text{C}$ and pressures up to 25 Mpa; however, PL-CZI either cracked when grinding or crushed during pressurization and indicated the former possesses excellent machinability and corrosion resistance [29, 30]. The EMF response and pressure response at various temperatures are shown in Fig. 6; the HP-CZI ceramic was sensitive to temperature and pressure; a steady EMF was established quickly as the temperature remained constant.

On the other hand, the PL-CZI ceramic either cracked during grinding or crushed during pressurization; therefore it could not be used in high-pressure hydrothermal systems. Regrettably, we have not found a hydrogen buffer suitable for use in high-pressure hydrothermal systems so it is impossible to verify the experimental data in theory and represents additional research we need to conduct to verify the next step.

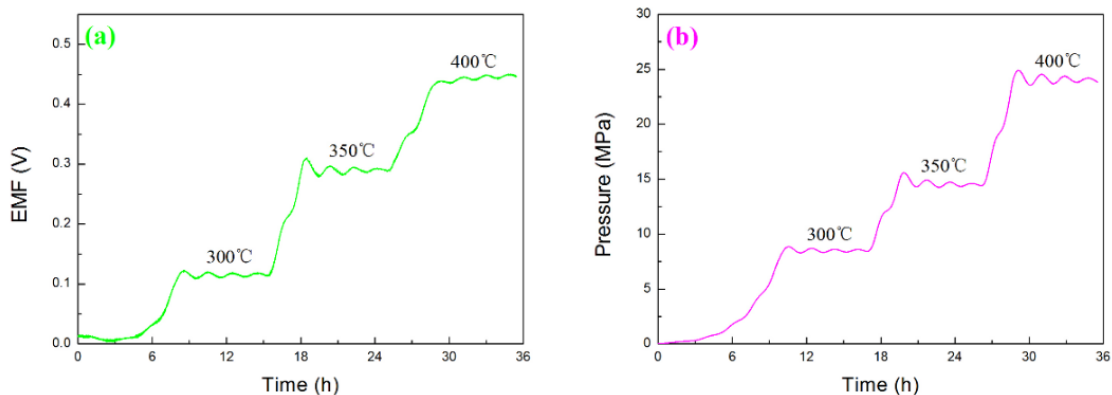


Figure 6. EMF response (a) and pressure response (b) at various temperatures when high pressure sintered CZI ceramic acts as an electrolyte and sealing material.

4. CONCLUSIONS

A novel sintering process has been successfully developed to obtain a high performance CZI ceramic. The CZI ceramic sintered at 0.4 GPa and 1000 °C exhibited a single orthorhombic perovskite structure. Compared with the CZI ceramic sintered under normal pressure, the HP-CZI ceramic had a more compact structure, higher conductivity, and most importantly, better machinability and corrosion resistance. Accordingly, the HP-CZI ceramic is regarded as one of the most promising electrolytes for in-situ measurement of H₂ in high-pressure hydrothermal fluids.

ACKNOWLEDGEMENTS

This work was supported by the National Key Research and Development Program of China [grant numbers 2016YFC0600104]; and “135” Program of the Institute of Geochemistry, Chinese Academy of Sciences.

References

1. K. Ding and W. Seyfried, *Chem. Rev.*, 107 (2007) 601.
2. N. Kishima, H. Sakai, *Earth Planet. Sci. Lett.*, 67 (1984) 79.
3. R. Farver, A. Yund, *Geochim. Cosmochim. Acta*, 54 (1990) 2953.
4. X. Zhang, R. Zhang, S. Hu and W. Yong, *Sci. China, Ser. E: Technol. Sci.*, 52 (2009) 2466.
5. K. Ding, W. Seyfried, *Science*, 272 (1996) 1634.

6. R. Zhang, X. Zhang and S.Hu, *Sens. Actuators, B*, 149 (2010) 143.
7. J. Peng, H. Li and D. Yan, *Ceram. Int.*, 45 (2019) 9310.
8. L. Duniyushkina, A. Pankratov, V. Gorelov and P. Tsiakaras, *Electrochim. Acta*, 202 (2016) 39.
9. J. Lang, J. You, X. Zhang, X. Luo and S. Zheng, *Ceram. Int.*, 44 (2018) 22176.
10. N. Fukatsu, N. Kurita, T. Yajima, K. Koide and T. Ohashi, *J. Alloys Compd.*, 231 (1995) 706.
11. T. Yajima, H. Iwahara, K. Koide and K. Yamamoto, *Sens. Actuators B*, 5 (1991) 145.
12. N. Kurita, N. Fukatsu, K. Ito and T. Ohashi, *J. Electrochem. Soc.*, 142 (1995) 1552.
13. H. Wang, Y. Han, R. Shi, L. Sheng, Q. Guan and J. Liu, *Int. J. Electrochem. Sci.*, 14 (2019) 755.
14. M. Goncalves, P. Maram, A. Navrotsky and R. Muccillo, *Ceram. Int.*, 42(2016) 13689.
15. J. Bao, H. Ohno, N. Kurita, Y. Okuyama and N. Fukatsu, *Electrochim. Acta*, 56 (2011) 1062.
16. J. Peng, H. Li and S. Lin, *J. Ceram. Soc. Jpn.*, 128 (2020) 62.
17. G. Róg, M. Dudek, A. Kozłowska-Róg, M. Bućko, *Electrochim. Acta*, 47 (2002) 4523.
18. L. Duniyushkina, A. Kuzmin, V. Kuimov, A. Khaliullina, M. Plekhanov, and N. Bogdanovich, *Russ. J. Electrochem.*, 53 (2017) 196.
19. X. Wang, T. Liu, J. Yu and L. Li, *J. Alloys Compd.*, 768 (2018) 838.
20. J. Lang, J. You, Zhang, F. Xiao, X. Luo and S. Zheng, *Ceram. Int.*, 44 (2018) 22176.
21. S. Hwang, G. Choi, *Solid State Ionics*, 179 (2008) 1042.
22. W. Huang, Y. Li, H. Li, Y. Ding and B. Ma, *Ceram. Int.*, 42 (2016) 13404.
23. P. Dahl, H. Lein, Y. Yu, J. Tolchard, T. Grande, M. Einarsrud, C. Kjolseth, T. Norby and R. Haugrud, *Solid State Ionics*, 182 (2011) 32.
24. S. Valkenberg, H. Bohn and W. Schilling, *Solid State Ionics*, 97 (1997) 511.
25. M. Islam, R. Davies and J. Gale, *Chem. Commun.*, 7 (2001) 661.
26. J. Han, Z. Wen, J. Zhang, Z. Gu and X. Xu, *Solid State Ionics*, 179 (2008) 1108.
27. Y. Gu, Z. Liu, J. Ouyang, F. Yan and Y. Zhou, *Electrochim. Acta*, 105 (2013) 547.
28. L. Dai, L. Wang, G. Shao and Y. Li, *Sens. Actuators B*, 173 (2012) 85.
29. L. Wang, H. Li, W. Liang, Y. Yin and Q. Liu, *Mater. Lett.*, 199 (2017) 61.
30. L. Zha, H. Li and N. Wang, *Mater. Lett.*, 234 (2019) 233.

© 2020 The Authors. Published by ESG (www.electrochemsci.org). This article is an open access article distributed under the terms and conditions of the Creative Commons Attribution license (<http://creativecommons.org/licenses/by/4.0/>).